Adsorption (2013) 19:643–652
DOI 10.1007/s10450-013-9487-6

Supercritical hydrogen adsorption in nanostructured solids with hydrogen density variation in pores

Jessica E. Sharpe · Nuno Bimbo · Valeska P. Ting · Andrew D. Burrows · Dongmei Jiang · Timothy J. Mays

Received: 31 October 2012 / Accepted: 24 January 2013 / Published online: 22 February 2013

Abstract Experimental excess isotherms for the adsorption of gases in porous solids may be represented by mathematical models that incorporate the total amount of gas within a pore, a quantity which cannot easily be found experimentally but which is important for calculations for many applications, including adsorptive storage. A model that is currently used for hydrogen adsorption in porous solids has been improved to include a more realistic density profile of the gas within the pore, and allows calculation of the total amount of adsorbent. A comparison has been made between different Type I isotherm equations embedded in the model, by examining the quality of the fits to hydrogen isotherms for six different nanoporous materials. A new Type I isotherm equation which has not previously been reported in the literature, the Unilan-*b* equation, has been derived and has also been included in this comparison study. These results indicate that while some Type I isotherm equations fit certain types of materials better than others, the Tóth equation produces the best overall quality of fit and also provides realistic parameter values when used to analyse hydrogen sorption data for a model carbon adsorbent.

Keywords Hydrogen adsorption · Porous solids · Isotherm equations

List of symbols

MOF	Metal–organic framework
PIM	Polymer of intrinsic microporosity
m_E	Excess mass of hydrogen
v_P	Pore volume
ρ_B	Bulk density
m_A^{max}	Limiting maximum uptake
θ_A	Fractional filling
wt %	Weight percent
P	Absolute pressure
b	Affinity parameter
Q	Enthalpic factor
b_0	Pre-exponential factor
R	Molar gas constant
T	Absolute temperature
bdc	Benzene-1,4-dicarboxylate
MIL	Matériaux de l'Institut Lavoisier
BET	Brunauer, Emmett and Teller
$m_{B(A)}$	Bulk hydrogen within the adsorbate
m_A	Absolute uptake
m_P	Total uptake
ρ_A	Adsorbate density
v_A	Adsorbate volume
M	Molar mass
Z	Compressibility factor
NIST	National Institute of Standards and Technology
$b_{(T)}$	Tóth affinity parameter
$c_{(T)}$	Tóth heterogeneity parameter
RMSR	Root mean square residual

Electronic supplementary material The online version of this article (doi:10.1007/s10450-013-9487-6) contains supplementary material, which is available to authorized users.

J. E. Sharpe
Department of Chemical Engineering, EPSRC Doctoral Training Centre, Centre for Sustainable Chemical Technologies, University of Bath, Bath BA27AY, UK

N. Bimbo · V. P. Ting · T. J. Mays (✉)
Department of Chemical Engineering, University of Bath, Bath BA27AY, UK
e-mail: T.J.Mays@bath.ac.uk

A. D. Burrows · D. Jiang
Department of Chemistry, University of Bath, Bath BA2 7AY, UK

b_1	Minimum value of b in a uniform distribution
b_2	Maximum value of b in a uniform distribution
Q_1	Minimum value of Q in a uniform distribution
Q_2	Maximum value of Q in a uniform distribution
$\theta(P,h)$	Local isotherm
h	Heterogeneity parameter
w	Substitution variable
$b_{(L)}$	Langmuir affinity parameter
$b_{(S)}$	Sips affinity parameter
$m_{(S)}$	Sips heterogeneity parameter
$b_{(GF)}$	Generalised Freundlich affinity parameter
q	Generalised Freundlich heterogeneity parameter
$b_{(JF)}$	Jovanović–Freundlich affinity parameter
$c_{(JF)}$	Jovanović–Freundlich heterogeneity parameter
α	Dubinin–Astakhov enthalpic factor
β	Dubinin–Astakhov entropic factor
$m_{(DA)}$	Adjustable parameter within the Dubinin–Astakhov equation
P_0	Vapour pressure
GCMC	Grand-canonical Monte Carlo

1 Introduction

Hydrogen shows great potential as an energy store; it is ubiquitous in the environment (in water and biomass), it can be sustainably produced, has the highest energy per unit mass of any chemical fuel, and only water is produced as a material product when releasing stored energy via heat engines or electrochemical devices such as fuel cells. However, a major issue with using hydrogen as an energy store is its very low energy density per unit volume. The density needs to be vastly increased to make it commercially viable, especially in applications where low mass, low volume stores are required, for example in light-duty land vehicles or to minimise plant footprints for static energy stores. Physisorption of molecular hydrogen (H_2) in nanoporous materials is one promising method of doing this and may improve on the conventional storage of liquid H_2 at low temperature (<33 K) or high pressure gas (up to 70 MPa). Adsorptive storage does not require a large energy input to recover the hydrogen from the adsorbent, unlike chemisorption, due to the relatively weak interaction between the adsorbent and the hydrogen, however, because of these weak interactions, low temperatures are required to store large quantities.

Materials that are commonly considered for gas storage include metal–organic frameworks (MOFs) (James 2003), zeolites (Bekkum 2001), activated carbons (Ströbel et al. 2006) and polymers of intrinsic microporosity (PIMs) (McKeown and Budd 2006). Analysis of these systems using adsorption models is very important for two main reasons. Firstly, models may be used to calculate the total amount of hydrogen within the system at any pressure and temperature (which cannot easily be measured experimentally) in order to compare the suitability of different materials for hydrogen storage. Secondly, models may be used to better understand fundamental aspects of the hydrogen adsorption process and hence guide materials design and selection, for example by finding the optimum pore sizes required to store the maximum quantity of hydrogen. The models must be framed to represent the excess mass of hydrogen, m_E, in order to fit to the Gibbs' excess isotherms obtained experimentally using volumetric or gravimetric gas sorption analysers. The excess refers to the additional amount of hydrogen in the pore as a result of the interactions between the hydrogen and the surface of the material. The basic model that is commonly utilized for hydrogen adsorption (Eq. 1) (Purewal et al. 2012; Czerny et al. 2005; Bimbo et al. 2011) assumes a uniform hydrogen density profile within the pore, and includes terms for the specific open pore volume, v_P, the mass density of the bulk hydrogen, ρ_B, the maximum amount of hydrogen that can be stored in the pore, m_A^{max}, and a Type I isotherm equation for fractional filling, Θ_A, as a function of pressure and temperature. Note that the factor of 100 is included in Eq. (1) in order to balance units, as all excess isotherms used have been converted to weight percent (wt %) relative to the dry activated (degassed) sample weight.

$$m_E = m_A^{max}\Theta_A - 100\rho_B v_P \tag{1}$$

There are many different Type I isotherm equations in the literature, both fundamental and empirical, many of which account for factors such as surface energy and pore size distributions (Do 1998; Jaroniec and Madey 1988; Rouquerol et al. 1998; Rudzinski and Everett 1992).

One of the earliest recognised isotherm equations was derived by Irving Langmuir in 1918, (Eq. 2), and is aptly named the Langmuir equation. It is an equation that calculates the coverage of adsorbed molecules on a surface with respect to pressure, at a fixed temperature (Langmuir 1918) and assumes an energetically homogenous surface.

$$\Theta_A = \frac{bP}{1+bP} \tag{2}$$

where P is the absolute pressure of the system, and b is the affinity parameter, a constant relating to the strength of adsorption onto the surface, which is usually assumed to follow an Arrhenius relationship (Arrhenius 1889):

$$b = b_0 \exp\left(\frac{Q}{RT}\right) \tag{3}$$

where Q is related to the enthalpy of adsorption, b_0 is the pre-exponential factor and relates to the entropy of

adsorption, R is the molar gas constant and T is the absolute temperature.

The simple Langmuir model has been extended to account for heterogeneous surfaces. Some well-known examples of these developments include the Tóth equation (Tóth 1971) and the Freundlich equation (Freundlich 1926) both of which have been used for hydrogen adsorption analysis by Gil et al. (2009), the Sips equation (Sips 1948) which has been used for analysis by Johansson et al. (2002), the modified Dubinin–Astakhov equation (Richard et al. 2009) which has been used for analysis by Poirier et al. (2006), and the Langmuir–Freundlich equation which has been used for analysis by Choi et al. (2003).

In order to explore the application and credibility of these and other adsorption models for extraction of a variety of parameters including the total hydrogen uptake, selected isotherm equations were applied to hydrogen uptake data for six different nanoporous materials as detailed in the following sections.

2 Experimental section

2.1 Materials and characterisation

TE7 carbon beads are a well characterised reference material, sourced from MAST Carbon International, Basingstoke, UK. They have a Brunauer, Emmett and Teller (BET) nitrogen specific surface area of 960 ± 50 $m^2\ g^{-1}$ (where the uncertainty here and elsewhere in this section refers to the standard deviation), obtained using the British Standard Method (British Standards Institution 1996) from low pressure nitrogen sorption measurements on a Micromeritics ASAP 2020 volumetric adsorption analyser at 77 K with a 60 min equilibration time (Hruzewicz-Kołodziejczyk et al. 2012). This material has a micropore volume of 0.43 ± 0.03 $cm^3\ g^{-1}$, evaluated from the Dubinin–Radushkevich method (Dubinin 1975), and a skeletal density of 1.90 ± 0.03 g cm^{-3}, measured using a He pycnometer (Micromeritics AccuPyc 1330). Samples were degassed for 8 h at 623 K prior to measurement of high pressure hydrogen sorption isotherms at 77, 89, 102, 120 and 150 K up to a maximum pressure of 14 MPa, using a Hiden HTP-1 Sieverts-type volumetric gas sorption analyser.

AX-21 activated carbon was sourced from Anderson Development Company Inc., Michigan, USA. This material has a BET nitrogen specific surface area of 2,448 ± 40 $m^2\ g^{-1}$, and a relatively broad pore size distribution compared to the TE7 carbon beads, with the majority of pores being around 1.4 nm, but with approximately 20 % of pores in the mesopore region (between 2 and 50 nm) (Zhou et al. 2000). Samples were degassed for 12 h at 473 K prior to measurement of high pressure hydrogen sorption isotherms at 90, 100, 110 and 120 K up to a maximum pressure of 18 MPa, using a Hiden HTP-1 Sieverts-type volumetric gas sorption analyser.

The chromium(III) terephthalate metal-organic framework $[Cr_3O(bdc)_3(OH,F)(H_2O)_2]$, MIL-101(Cr), (where MIL stands for 'Matériaux de l'Institut Lavoisier', and bdc is benzene-1,4-dicarboxylate) was prepared by adapting the method reported previously by Jiang et al. (2011). 0.33 g of terephthalic acid $[C_6H_4\text{-}1,4\text{-}(CO_2H)_2]$ were added to 0.8 g chromium(III) nitrate nonahydrate $[Cr(NO_3)_3{\cdot}9H_2O]$ in a Teflon-lined autoclave, with 10 mL distilled water and a stirrer bar. This was heated to 453 K and left for 8 h, before cooling overnight to room temperature. The white powder formed was washed with deionised water and vacuum filtered to form a blue/green suspension, which was centrifuged three times in water for 10 min each time at 11,000 rpm and left to dry, resulting in a green solid. Following the synthesis, the solvent was removed from the pores by drying in a vacuum oven, and then degassing at 423 K for 4 h. MIL-101(Cr) is a rigid, well-studied MOF with pore sizes ranging between 2.9 and 3.4 nm (Férey et al. 2005), and a BET nitrogen surface area of 2,887 ± 106 $m^2\ g^{-1}$. Samples were degassed for 4 h at 423 K prior to measurement of high pressure hydrogen sorption isotherms at 77, 90, 100 and 110 K up to a maximum pressure of 18 MPa, using a Hiden HTP-1 Sieverts-type volumetric gas sorption analyser.

[Al(OH)(bdc)], MIL-53(Al), was prepared by adapting the previously reported synthetic procedure (Loiseau et al. 2004). 0.165 g of terephthalic acid $[C_6H_4\text{-}1,4\text{-}(CO_2H)_2]$ were added to 0.376 g aluminium(III) nitrate nonahydrate $[Al(NO_3)_3{\cdot}9H_2O]$ in a Teflon-lined autoclave, with 10 mL distilled water and a stirrer bar. This was heated to 493 K and left for 8 h, before cooling overnight to room temperature. The white powder formed was then washed with acetone and vacuum filtered to form a clear liquid, which was centrifuged three times in acetone for 10 min each time at 11,000 rpm and left to dry, resulting in a white solid. The solvent was then removed from the pores by drying in a vacuum oven, and then degassing at 423 K for 4 h. This material was chosen due to its propensity for breathing or pore distortion (Boutin et al. 2009; Serre et al. 2007; Neimark et al. 2011). This behavior is thought to occur with changes in either temperature, pressure, or introduction of a guest molecule, which causes the pores to stretch, reducing the volume within. The pore sizes in MIL-53(Al) vary between 1.7–2.1 nm, and 1.3–0.7 nm, between the large pore and narrow pore structures respectively (Liu et al. 2008), and the material has a BET nitrogen surface area of 1,118 ± 47 $m^2\ g^{-1}$. Samples were degassed for 4 h at 423 K prior to measurement of high pressure hydrogen sorption isotherms at 77, 90, 100, 110 and 120 K up to a maximum pressure of

18 MPa, using a Hiden HTP-1 Sieverts-type volumetric gas sorption analyser.

NOTT-101 is a copper-based MOF, with the formula Cu_2(tptc) (where tptc is terphenyl-3,3″,5,5″-tetracarboxylate), and was originally synthesised in Nottingham in 2006 (Lin et al. 2006). It has an average pore size of 0.65 nm, and a BET surface area of 2,510 m^2 g^{-1}. The hydrogen sorption data was provided by Anne Dailly from General Motors Research and Development Centre (GM Research and Development Centre, Warren, MI, USA) from hydrogen isotherm measurements at 50, 60, 70, 77 and 87 K (Poirier and Dailly 2009).

Zeolitic imidazolate framework 8 (ZIF-8) is a MOF that is topologically isomorphic with a sodalite (SOD) zeolite. It consists of a tetrahedrally-coordinated zinc centre linked by imidazolate, and the pores are 1.16 nm in diameter, connected by small apertures of 0.34 nm. ZIF-8 was first reported in 2006 (Park et al. 2006), and the hydrogen sorption isotherms were obtained from the literature using EnGauge data-reading software at 50, 60, 77, 100 and 125 K (Zhou et al. 2007).

2.2 High pressure hydrogen sorption measurements

High pressure volumetric gas sorption studies were conducted on a Hiden HTP-1 Sieverts-type volumetric gas sorption analyser up to pressures of 20 MPa. High purity hydrogen was used for all of the measurements (99.99996 %, BIP-Plus from Air Products), with the 77 K isotherms using a liquid nitrogen bath for temperature control. Prior to each measurement, the samples (typically 100 mg) were degassed in order to remove impurities from surfaces and pores, applying a minimum equilibration time of 12 min. All isotherms presented in this paper measured using the HTP-1 were fully reversible, and repeat isotherms were reproduced to within 0.3 % of the measured amounts adsorbed. All isotherms are reported as excess hydrogen uptake in wt % relative to the degassed sample weight.

2.3 Data analysis

All non-linear fitting was carried out using the Origin 8.5 Pro software (OriginLab Corporation, Massachusetts, USA). This programme uses a Levenberg–Marquardt method of non-linear fitting (Marquardt 1963), which combines the steepest-descent method and the Gauss–Newton method to adjust the parameter values to achieve the minimum χ^2_{red} value (a measure of the quality of fit). Up to 400 fitting iterations were carried out with a tolerance of 10^{-9}.

3 Mathematical model

An improvement on the general model (Eq. 1) is described, taking into account density variation of fluid within pores. This allows for an adsorbate (adsorbed phase) with a higher density, ρ_A, than that of the bulk gas, ρ_B (Fig. 1). The sections of the graph of the density profile of the hydrogen in the pore (Fig. 1) containing vertical lines represents m_E. The sections containing the vertical lines plus the sections containing the diagonal lines (where the section containing the diagonal lines indicates the amount of hydrogen that would be within the area of the adsorbate if there were no interactions with the surface, $m_{B(A)}$) represents the absolute amount of hydrogen, which is the total amount of hydrogen within the adsorbate, m_A. The sections containing the vertical lines, plus the sections containing the diagonal lines, plus the section containing the horizontal dashed lines (where the section containing the horizontal dashed lines indicates the amount of bulk hydrogen) represents the total amount of hydrogen within the pores, m_P (Schlichtenmayer and Hirscher 2012).

3.1 Derivation of the model

As the excess hydrogen is equal to the total amount of hydrogen within the adsorbate minus the bulk amount of hydrogen within the adsorbate, it can be stated that

$$m_E = m_A - m_{B(A)} \tag{4}$$

where

$$m_A = \rho_A v_A \tag{5}$$

where ρ_A is the density of the adsorbate, and v_A is the volume of the adsorbate, and

$$m_{B(A)} = \rho_B v_A \tag{6}$$

Therefore, substituting Eqs. (5) and (6) into Eq. (4) gives

$$m_E = \rho_A v_A - \rho_B v_A \tag{7}$$

which can be simplified to give

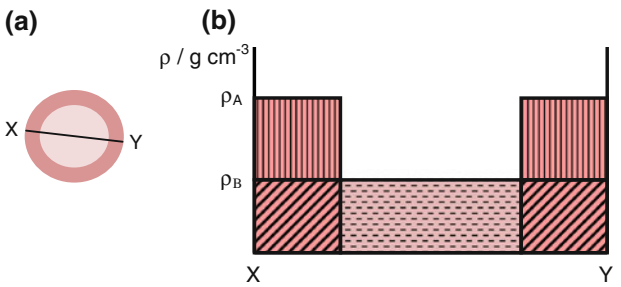

Fig. 1 Assumed hydrogen density profile within a pore. **a** A cross-sectional diagram of the pore. **b** The corresponding density profile, with the *x* axis representing the cross section of the pore, where ρ_A represents the mass density of the adsorbate, and ρ_B represents the mass density of the bulk hydrogen (Color figure online)

$$m_E = (\rho_A - \rho_B)v_A \tag{8}$$

Note that the total amount in the pore is

$$m_P = m_E + \rho_B v_P \tag{9}$$

The bulk adsorptive density can be determined using an equation of state

$$\rho_B = \frac{1}{Z}\frac{PM}{RT} \tag{10}$$

where M is molar mass and Z is the compressibility factor (for an ideal gas, $P \to 0$, $Z \to 1$). We use a rational approximation (Bimbo et al. 2011) to the Leachman equation of state for hydrogen (Leachman et al. 2009), which is available through the National Institute of Standards and Technology (NIST) website (2011).

A fractional filling term, Θ_A, is defined as,

$$\Theta_A = \frac{v_A}{v_P} \tag{11}$$

We assume Θ_A is of the form of an IUPAC Type I isotherm. Therefore, substituting Eqs. (10) and (11) into Eq. (8), the following equation has been derived

$$m_E = \left(\rho_A - \frac{1}{Z}\frac{PM}{RT}\right)100 v_P \Theta_A \tag{12}$$

The multiplier of 100 has been included into the equation in order to balance units, as described in the "Introduction" section. Equation (12) is the model framework for analysing experimental excess adsorption isotherms. Note that at low pressure $m_E = m_A = \rho_A\, \Theta_A\, v_P$ which would lead to difficulties in obtaining separate, stable estimates of the product $\rho_A\, v_P$ from fitting to data.

3.2 A direct comparison between the two equations

A comparison between the average density model (Eq. 1) and the model incorporating a density variation (Eq. 12) has been made, shown here using the TE7 carbon beads and the Tóth isotherm equation (Eq. 13) as an example:

$$\Theta_A = \frac{b_{(T)}P}{\left(1 + \left(b_{(T)}P\right)^{c_{(T)}}\right)^{\frac{1}{c_{(T)}}}} \tag{13}$$

where $b_{(T)}$ is the Tóth affinity parameter and $c_{(T)}$ is the Tóth heterogeneity parameter.

The root mean square residual (RMSR), explained in the Online Resource, has been used to compare the quality of the fits, with lower RMSR indicating better fit (Fig. 2):

Bias was also examined for both of the sets of fits, as well as the use of other isotherm equations as described in the Online Resource. While both models fit the data with very similar RMSR values, the improved model was chosen for detailed study as it explicitly accounts for adsorbate density.

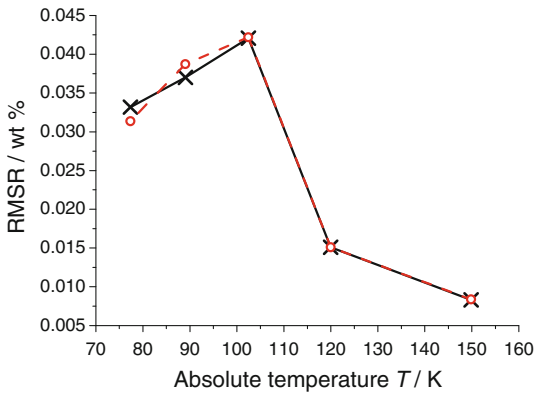

Fig. 2 A comparison of the average density model and the model incorporating a density variation, using the Tóth equation, and fit to isotherms from the TE7 carbon beads. Straight lines were used to join the points to guide the eye, with the dotted line linking the open circles of the model incorporating the density variation (Eq. 12), and the solid line linking the crosses of the average density model (Eq. 1) (Color figure online)

3.3 Unilan-*b* equation

In order to extend and further test the analysis a new isotherm equation was introduced, the Unilan-*b* (Eq. 14). This new equation is similar to the more familiar Unilan-*Q* equation (Eq. 15) (Honig and Reyerson 1952), but assumes a different heterogeneity function.

$$\Theta_A = 1 - \frac{1}{P(b_2 - b_1)}\ln\left(\frac{1 + b_2 P}{1 + b_1 P}\right) \tag{14}$$

$$\Theta_A = \frac{RT}{Q_2 - Q_1}\ln\left(\frac{1 + b_0 \exp\left(\frac{Q_2}{RT}\right)P}{1 + b_0 \exp\left(\frac{Q_1}{RT}\right)P}\right) \tag{15}$$

where b_1 and b_2 are the minimum and maximum values of the affinity parameter b respectively and Q_1 and Q_2 are the minimum and maximum values of the energy parameter Q respectively.

The Unilan-*Q* equation uses a uniform distribution function with respect to Q, whereas the Unilan-*b* equation uses a uniform distribution with respect to b (Fig. 3), with the two parameters being related according to Eq. (3). A full derivation of the Unilan-*b* equation is given in the Online Resource.

The Unilan-*b* equation follows Henry's Law in the limit of low pressure, saturates to unity at high pressure, and reduces to the Langmuir equation when b_2 approaches b_1 (in which case $f(b)$ approaches the Dirac delta function).

There are notable benefits arising from the new Unilan-*b* equation compared with the original Unilan-*Q* equation. Firstly, b is considered as the single adjustable parameter since A and Q in the Arrhenius equation may be correlated via the 'compensation effect'(Wilson and Galwey 1973). Secondly, the Unilan-*b* equation is far simpler to implement and has fewer parameters than the Unilan-*Q* equation.

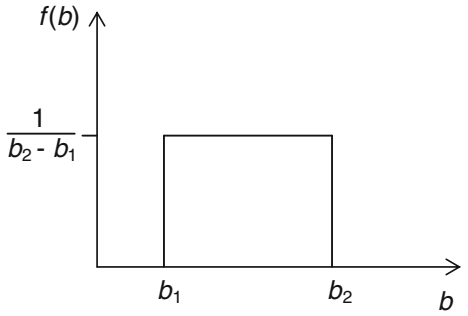

Fig. 3 The distribution of the affinity parameter for the Unilan-*b* equation. *b* is in inverse units of pressure, and f(*b*) is in units of pressure

The most preferable equation to use for the comparison of different materials for hydrogen uptake would be one that fits the data, but with the fewest number of parameters. This follows Occam's razor, which states that when choosing between models, the one with the fewest assumptions is preferred.

4 Results and discussion

4.1 Selection of variables

Equation (12) was used as the model for analysis of the experimental excess hydrogen adsorption data for the six different nanoporous materials described in Sect. 2.1. Initially eight different Type I isotherms were tested for Θ_A. The materials were chosen to include a range of different types of materials with different pore sizes and volumes, some of which were synthesised and analysed in Bath, some of which were sourced externally and then analysed in-house, and some of which the information was collected from published literature. Different isotherm equations, most of which have been used in the literature to model hydrogen adsorption, were chosen to test our analysis. The majority of these equations are well known Type I equations, each embedding a range of characteristic parameters. The eight different isotherm equations used are summarised in Table 1.

Table 1 A summary of the Type I isotherm equations used within the study

Name (reference)	Equation and explanation of terms	Number of parameters
Langmuir (Langmuir 1918)	$\Theta_A = \frac{b_{(L)}P}{1+b_{(L)}P}$ (2) $b_{(L)}$ is the Langmuir affinity parameter	1
Tóth (Tóth 1971)	$\Theta_A = \frac{b_{(T)}P}{\left(1+\left(b_{(T)}P\right)^{c(T)}\right)^{\frac{1}{c(T)}}}$ (13)	2
Sips (Sips 1948)	$\Theta_A = \frac{\left(b_{(S)}P\right)^{\frac{1}{m(S)}}}{1+\left(b_{(S)}P\right)^{\frac{1}{m(S)}}}$ (16) $b_{(S)}$ is the Sips affinity parameter $m_{(S)}$ is the Sips heterogeneity parameter	2
Generalised Freundlich (Sips 1950)	$\Theta_A = \left(\frac{b_{(GF)}P}{1+b_{(GF)}P}\right)^q$ (17) $b_{(GF)}$ is the Generalised Freundlich affinity parameter q is the Generalised Freundlich heterogeneity parameter	2
Jovanović–Freundlich (Quiñones and Guiochon 1996)	$\Theta_A = 1 - \exp(-\left(b_{(JF)}P\right)^{c_{(JF)}})$ (18) $b_{(JF)}$ is the Jovanović–Freundlich affinity parameter $c_{(JF)}$ is the Jovanović–Freundlich heterogeneity parameter	2
Dubinin–Astakhov (Richard et al. 2009)	$\Theta_A = \exp\left(\frac{RT}{\alpha+\beta T}\right)^{m(DA)} \ln\left(\frac{P_0}{P}\right)^{m(DA)}$ (19) α is the Dubinin–Astakhov enthalpic factor β is the Dubinin–Astakhov entropic factor $m_{(DA)}$ is an adjustable parameter in the Dubinin–Astakhov equation P_0 is the vapour pressure (non-existent for a supercritical fluid, therefore a parameter from the fit)	4
Unilan-*Q* (Honig and Reyerson 1952)	$\Theta_A = \frac{RT}{Q_2-Q_1} \ln\left(\frac{1+b_0 \exp\left(\frac{Q_2}{RT}\right)P}{1+b_0 \exp\left(\frac{Q_1}{RT}\right)P}\right)$ (15)	3
Unilan-*b* (this work)	$\Theta_A = 1 - \frac{1}{P(b_2-b_1)} \ln\left(\frac{1+b_2P}{1+b_1P}\right)$ (14)	2

4.2 Fitting methodology

The first step in the analysis involved fitting Eq. (12) for a selected Type I filling function Θ_A to each individual isotherm for all of the materials separately, constituting a total of 216 fits. Estimated values of v_P and ρ_A and of parameters of the Type I isotherm equation for a given material were then plotted as a function of temperature. These plots indicated that neither pore volume nor the adsorbate density depended on temperature and were therefore assumed to be constants for a given Type I isotherm and material. It should be noted that implicit in all these fits was an assumption that none of the parameters were dependent upon pressure. In future work the possible pressure dependence of v_P and ρ_A will be explored in more detail.

Global fits (fits over the entire temperature range for each material assuming v_P and ρ_A to be constant, but allowing each parameter within the Type I isotherm equations to vary) were then conducted on the variable

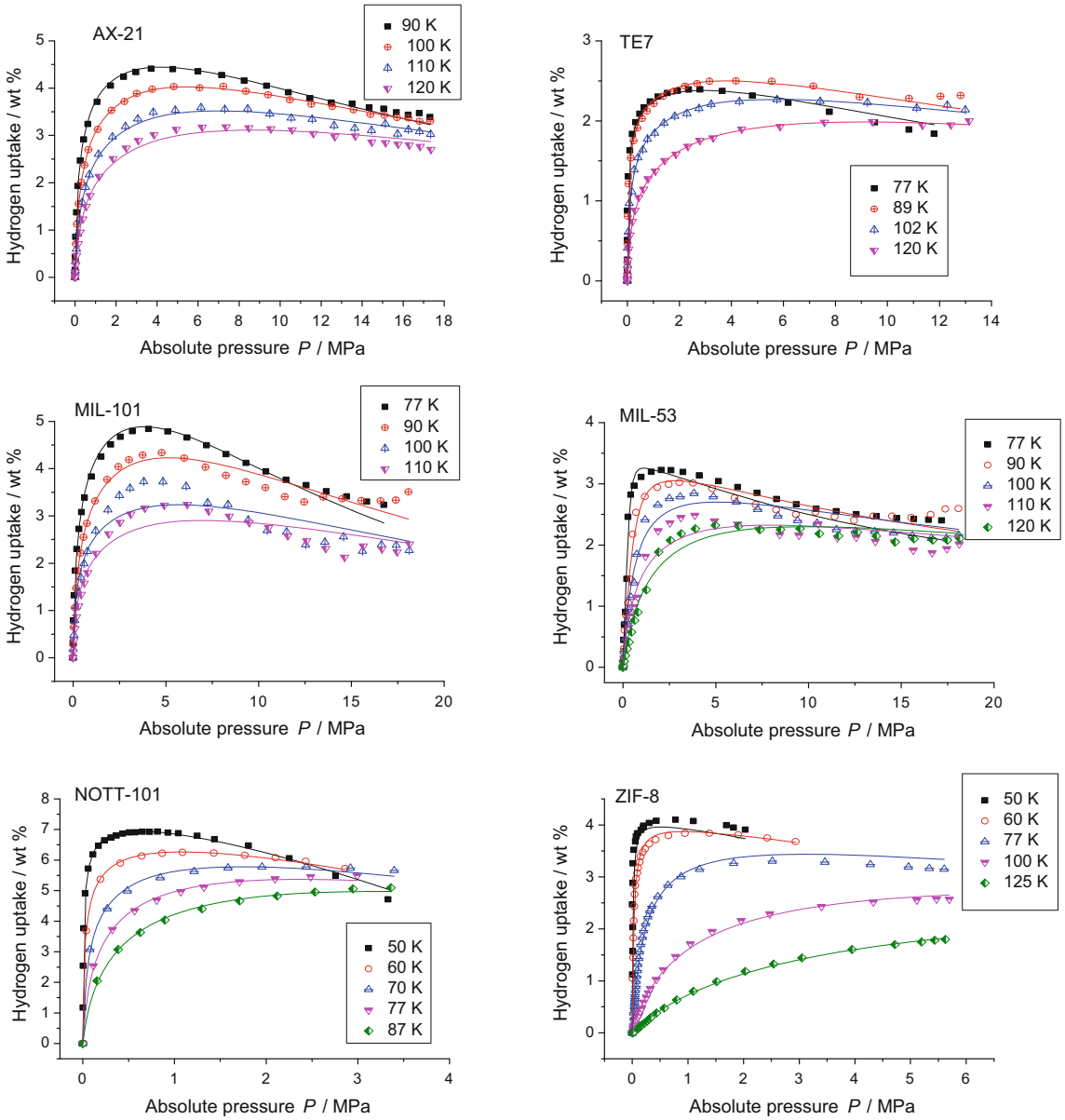

Fig. 4 Global fits using the Tóth equation for all adsorbents. The *points* indicate the experimental data, with the *lines* showing the fits (Color figure online)

Table 2 Parameter values estimated from the global fits using the Tóth model for H_2 isotherms on the TE7 carbon beads

Temperature / K	$b_{(T)}$ / MPa^{-1}	$c_{(T)}$ / –	v_P / $cm^3\ g^{-1}$	ρ_A / $g\ cm^{-3}$
77	12,300 ± 6,460	0.200 ± 0.0140	0.469 ± 0.0544	0.100 ± 0.00448
89	927 ± 437	0.245 ± 0.0197		
102	102 ± 33.2	0.275 ± 0.0197		
120	10.7 ± 2.25	0.316 ± 0.0198		

Uncertainties are standard errors

temperature hydrogen sorption datasets for each material for each Type I isotherm equation within the model. These global fits are in the Online Resource, except for the fits using the Tóth isotherm equation, which are shown, for illustration of our approach, in Fig. 4. Table 2 shows the parameter values for the global fit of the Tóth isotherm equation to the H_2 adsorption data for the TE7 carbon beads, which is the most well-characterised material of the

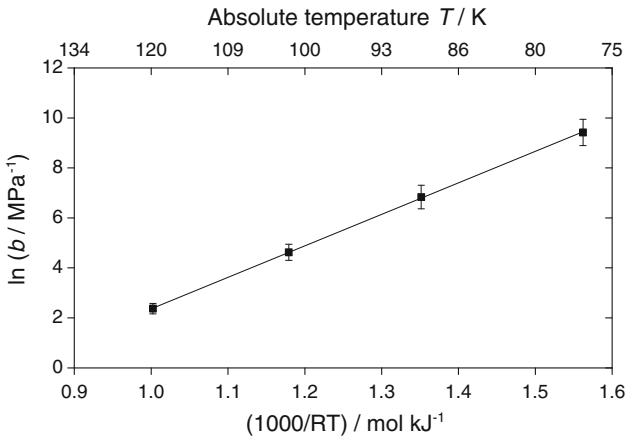

Fig. 5 An Arrhenius plot for b for the Tóth fit to the TE7 carbon beads. The line of best fit is created using a linear least squares method. The *error bars* are standard errors

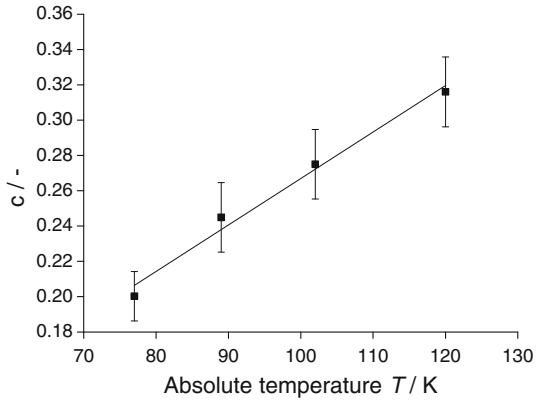

Fig. 6 Values of c with temperature refined from the fit using the Tóth model on the isotherms of the TE7 carbon beads. The line of best fit is created using a linear least squares method. The *error bars* are standard errors

six materials examined. Parameter values for the Tóth global fits for the remaining five materials are in the Online Resource for comparison.

Figure 5 shows that the Tóth affinity parameter $b_{(T)}$ depends on T according to an Arrhenius relationship, as expected from Eq. (3). The c parameter appears to increase with increasing T (Fig. 6). This is not unexpected as the effects of heterogeneity reduce with increasing T (in the limit $c \rightarrow 1$, the heterogeneous Tóth isotherm approaches the homogeneous Langmuir isotherm). The value of v_P in Table 2 is very close to the pore volume of 0.43 $cm^3\ g^{-1}$ obtained from the N_2 isotherm at 77 K using the Dubinin–Radushkevich method. Remarkably, ρ_A is estimated to be about 0.1 $g\ cm^{-3}$, indicating a solid-like density of hydrogen within the pores (Silvera 1980). The presence of solid-like H_2 in nanopores has been predicted previously using Grand-Canonical Monte Carlo (GCMC) simulations (Jagiello et al. 2006; Wang and Johnson 1998). Overall, the Tóth model produced realistic values and trends for all of the parameters when used to fit to H_2 adsorption data for the TE7 carbon beads in the temperature and pressure ranges examined.

4.3 Comparison of the quality of fit between Type I isotherms

The RMSR was used as a measure of the quality of fit for each of the eight isotherm models for each of the six adsorbents. Figure 7 shows cumulative RMSR data for each model, and Fig. 8 shows individual RMSR data for each model of the six materials.

Both Figs. 7 and 8 show the same information, represented in different ways in order to emphasise different features. Figure 7 shows that overall, the Langmuir and the Unilan-b equations have the worst fits to the data in terms

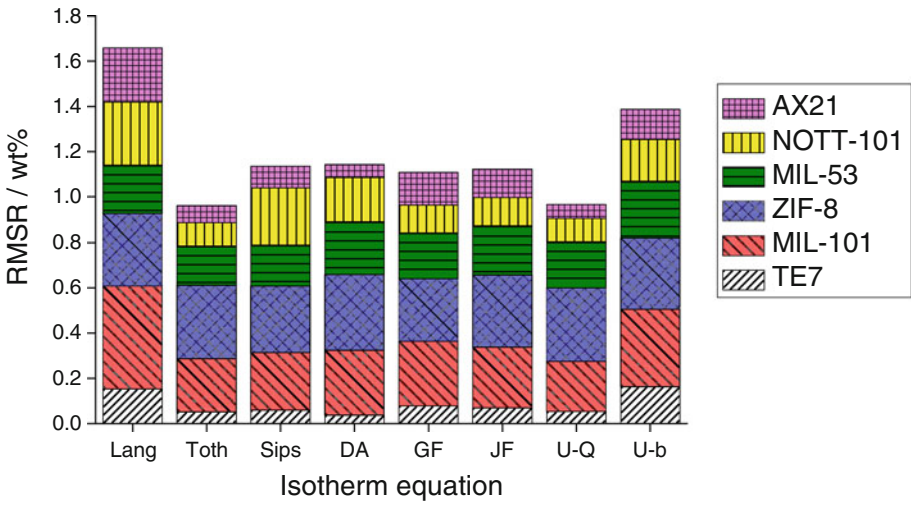

Fig. 7 Cumulative RMSR for each isotherm equation, where Lang = Langmuir, DA = Dubinin-Astakhov, GF = Generalised Freundlich, JF = Jovanović-Freundlich, U-Q = Unilan-Q and U-b = Unilan-b (Color figure online)

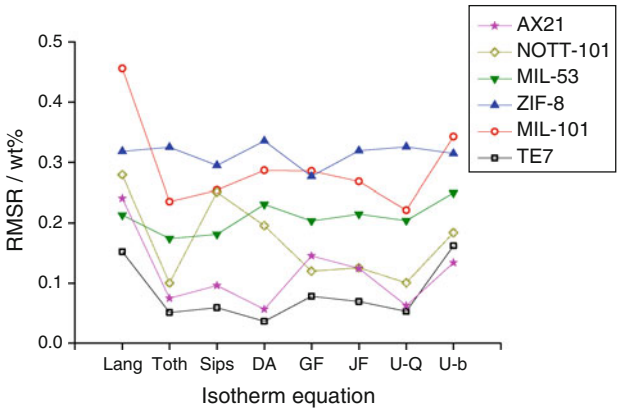

Fig. 8 RMSR for each isotherm equation and each material. *Straight lines* are drawn between points to guide the eye (Color figure online)

of RMSR, and the Tóth and the Unilan-*Q* have the best fits to the data, with the other four equations having relatively similar quality of fits.

However, Fig. 8 shows that even though the Tóth has the best fit overall to the data, it is not the best equation to use for every material. For example, the Sips equation and the Generalized Freundlich equation both have better fits to the ZIF-8 data than the Tóth equation. It also shows that generally, all of the equations fit better to the carbon materials (TE7 and AX-21) then the MOFs, and the worst fits are to the ZIF data. This result could be affected by the capacity of the materials, as higher capacities could result in higher RMSR values. Another point to note from Fig. 8 is that some equations show much higher RMSRs for certain materials than expected. For example, the Sips and the Dubinin–Astakhov equations show much higher RMSRs for NOTT-101 in comparison to the other equations than they do for other materials.

5 Conclusions

A new model that incorporates a more realistic description of fluid density inside pores has been derived and results in fits to experimental excess adsorption isotherm data to a very similar standard as the former average density model, but is able to distinguish between the amounts of hydrogen adsorbate and bulk hydrogen within pores. This new description (Eq. 12) could prove useful not only for the analysis of supercritical hydrogen sorption data, but could also be applied to data from other supercritical adsorptives such as methane and carbon dioxide. The remarkable observation of solid-like densities for hydrogen adsorbate in a TE7 carbon bead material suggests future positive options for hydrogen storage in similar materials to meet demanding targets set, for example, by the U.S. Department of Energy (U.S. Department of Energy 2009).

Statistical comparison of different Type I isotherm models for the pore filling function, Θ_A, in the new model suggests that the Tóth equation (one heterogeneous version of the Langmuir equation) may, on average, be the best choice in terms of quality of fit for hydrogen adsorption isotherms over a range of nanoporous materials. However, this is not a universal trend; for example the relatively simple new Unilan-*b* equation appears to be a good model for adsorption on the ZIF-8 material, and the reasons why different isotherms produce different results may well be due to differences in quantities such as pore shapes and sizes, rigidity of the materials and adsorption mechanisms implied in the different isotherm equations. One aspect that will be studied in more detail using the new model, which will be reported in due course, is the pressure and temperature dependence of adsorbate density and pore volume.

Acknowledgments JES thanks the UK Engineering and Physical Sciences Research Council (EPSRC) Doctoral Training Centre in Sustainable Chemical Technologies at the University of Bath, and also to Dr Agata Godula-Jopek from the EADS Innovation Works, Munich, Germany for financial support. NB and TJM thank the EPSRC for funding via the SUPERGEN United Kingdom Sustainable Hydrogen Energy Consortium (UK-SHEC, EP/J016454/1), VPT thanks the University of Bath for funding via an EPSRC Development Fund grant and a Prize Research Fellowship, and VPT and TJM thank the EPSRC for supporting the latter stages of this work via its Delivery Fund at the University of Bath and the SUPERGEN Hydrogen and Fuel Cells Hub (EP/E040071/1). JES, NB and VPT thank the Organising Committee of the 8th International Symposium of the Effects of Surface Heterogeneity in Adsorption and Catalysis on Solids (ISSHAC-8, Aug 2012, Kraków, Poland) for the opportunity to present this work as an oral presentation and for subsidising registration for the conference. The authors thank Anne Dailly (Chemical Sciences and Materials Systems Laboratory, General Motors Global Research and Development, Warren, MI, U.S) for providing the NOTT-101 data. ADB and DJ thank the EPSRC for funding (EP/H046305/1).

References

Arrhenius, S.: Uber die Reaktionsgeschwindigkeit bei der Inversion von Rohrzucker durch Säuren. Z. Physik. Chem. **4**, 226 (1889)

Bekkum, H.V.: Introduction to Zeolite Science and Practice, vol. 137. Elsevier, Amsterdam (2001)

Bimbo, N., Ting, V.P., Hruzewicz-Kolodziejczyk, A., Mays, T.J.: Analysis of hydrogen storage in nanoporous materials for low carbon energy applications. Faraday Discuss. **151**, 59–74 (2011)

Boutin, A., Springuel-Huet, M.-A., Nossov, A., Gédéon, A., Loiseau, T., Volkringer, C., Férey, G., Coudert, F.-X., Fuchs, A.H.: Breathing transitions in MIL-53(Al) metal–organic framework upon xenon adsorption. Angew. Chem. Int. Edit. **48**(44), 8314–8317 (2009)

British Standards Institution: Determination of the specific surface area of powders-part 1: BET method of gas adsorption for solids (including porous materials). In: [BS 4359-1, ISO 9277:1995]. British Standards Institution (1996)

Choi, B.-U., Choi, D.-K., Lee, Y.-W., Lee, B.-K., Kim, S.-H.: Adsorption equilibria of methane, ethane, ethylene, nitrogen, and

hydrogen onto activated carbon. J. Chem. Eng. Data **48**(3), 603–607 (2003)
Czerny, A.M., Bénard, P., Chahine, R.: Adsorption of nitrogen on granular activated carbon: experiment and modeling. Langmuir **21**(7), 2871–2875 (2005)
Do, D.D.: Adsorption Analysis: Equilibria and Kinetics, vol. 2. Series on Chemical Engineering. Imperial College Press, London (1998)
Dubinin, M.M.: In: Cadenhead, D.A. (ed.) Progress in Surface and Membrane Science, vol. 9. Academic Press, New York (1975)
Férey, G., Mellot-Draznieks, C., Serre, C., Millange, F., Dutour, J., Surblé, S., Margiolaki, I.: A chromium terephthalate-based solid with unusually large pore volumes and surface area. Science **309**(5743), 2040–2042 (2005)
Freundlich, H.: Colloid & Capillary Chemistry. Methuen & Co. Ltd., London (1926)
Gil, A., Trujillano, R., Vicente, M.A., Korili, S.A.: Hydrogen adsorption by microporous materials based on alumina-pillared clays. Int. J. Hydrogen Energy **34**(20), 8611–8615 (2009)
Honig, J.M., Reyerson, L.H.: Adsorption of nitrogen, oxygen and argon on rutile at low temperatures; applicability of the concept of surface heterogeneity. J. Phys. Chem. **56**(1), 140–144 (1952)
Hruzewicz-Kołodziejczyk, A., Ting, V.P., Bimbo, N., Mays, T.J.: Improving comparability of hydrogen storage capacities of nanoporous materials. Int. J. Hydrogen Energy **37**(3), 2728–2736 (2012)
International Energy Agency: World Energy Outlook 2010. In: OECD: Organisation for Economic Co-operation and Development. World Energy Outlook, Paris (2010)
Jagiello, J., Ansón, A., Martínez, M.T.: DFT-based prediction of high-pressure H_2 adsorption on porous carbons at ambient temperatures from low-pressure adsorption data measured at 77 K. J. Phys. Chem. B **110**(10), 4531–4534 (2006)
James, S.L.: Metal-organic frameworks. Chem. Soc. Rev. **32**(5), 276–288 (2003)
Jaroniec, M., Madey, R.: Physical Adsorption on Heterogeneous Solids. Elsevier, Amsterdam (1988)
Jiang, D., Burrows, A.D., Edler, K.J.: Size-controlled synthesis of MIL-101(Cr) nanoparticles with enhanced selectivity for CO_2 over N_2. Cryst. Eng. Commun. **13**(23), 6916–6919 (2011)
Johansson, E., Hjörvarsson, B., Ekström, T., Jacob, M.: Hydrogen in carbon nanostructures. J. Alloy. Compd. **330–332**, 670–675 (2002)
Langmuir, I.: The adsorption of gases on plane surfaces of glass, mica and platinum. J. Am. Chem. Soc. **40**(9), 1361–1403 (1918)
Leachman, J.W., Jacobsen, R.T., Penoncello, S.G., Lemmon, E.W.: Fundamental equations of state for parahydrogen, normal hydrogen, and orthohydrogen. J. Phys. Chem. Ref. Data **38**, 721–728 (2009)
Lin, X., Jia, J., Zhao, X., Thomas, K.M., Blake, A.J., Walker, G.S., Champness, N.R., Hubberstey, P., Schröder, M.: High H_2 adsorption by coordination-framework materials. Angew. Chem. Int. Edit. **45**(44), 7358–7364 (2006)
Liu, Y., Her, J.-H., Dailly, A., Ramirez-Cuesta, A.J., Neumann, D.A., Brown, C.M.: Reversible structural transition in MIL-53 with large temperature hysteresis. J. Am. Chem. Soc. **130**(35), 11813–11818 (2008)
Loiseau, T., Serre, C., Huguenard, C., Fink, G., Taulelle, F., Henry, M., Bataille, T., Férey, G.: A rationale for the large breathing of the porous aluminum terephthalate (MIL-53) upon hydration. Chem. Eur. J. **10**(6), 1373–1382 (2004)
Marquardt, D.W.: An algorithm for least-squares estimation of nonlinear parameters. J. Soc. Ind. Appl. Math. **11**(2), 431–441 (1963)
McKeown, N.B., Budd, P.M.: Polymers of intrinsic microporosity (PIMs): organic materials for membrane separations, heterogeneous catalysis and hydrogen storage. Chem. Soc. Rev. **35**(8), 675–683 (2006)
National Institute of Standards and Technology: NIST Chemistry WebBook. http://webbook.nist.gov/ (2011). Accessed 18/09/2012
Neimark, A.V., Coudert, F.O.-X., Triguero, C., Boutin, A., Fuchs, A.H., Beurroies, I., Denoyel, R.: Structural transitions in MIL-53 (Cr): view from outside and inside. Langmuir **27**(8), 4734–4741 (2011)
Park, K.S., Ni, Z., Côté, A.P., Choi, J.Y., Huang, R., Uribe-Romo, F.J., Chae, H.K., O'Keeffe, M., Yaghi, O.M.: Exceptional chemical and thermal stability of zeolitic imidazolate frameworks. Proc. Natl. Acad. Sci. **103**(27), 10186–10191 (2006)
Poirier, E., Dailly, A.: Thermodynamic study of the adsorbed hydrogen phase in Cu-based metal-organic frameworks at cryogenic temperatures. Energy Environ. Sci. **2**(4), 420–425 (2009)
Poirier, E., Chahine, R., Bénard, P., Lafi, L., Dorval-Douville, G., Chandonia, P.A.: Hydrogen adsorption measurements and modeling on metal-organic frameworks and single-walled carbon nanotubes. Langmuir **22**(21), 8784–8789 (2006)
Purewal, J., Liu, D., Sudik, A., Veenstra, M., Yang, J., Maurer, S., Müller, U., Siegel, D.J.: Improved hydrogen storage and thermal conductivity in high-density MOF-5 composites. J. Phys. Chem. C **116**(38), 20199–20212 (2012)
Quiñones, I., Guiochon, G.: Derivation and application of a Jovanovic–Freundlich isotherm model for single-component adsorption on heterogeneous surfaces. J. Colloid Interface Sci. **183**(1), 57–67 (1996)
Richard, M.A., Bénard, P., Chahine, R.: Gas adsorption process in activated carbon over a wide temperature range above the critical point. Part 1: modified Dubinin–Astakhov model. Adsorption **15**(1), 43–51 (2009)
Rouquerol, J., Rouquerol, F., Sing, K.S.W.: Absorption by Powders and Porous Solids. Elsevier, Amsterdam (1998)
Rudzinski, W., Everett, D.H.: Adsorption of Gases on Heterogeneous Surfaces. Academic Press, London (1992)
Schlichtenmayer, M., Hirscher, M.: Nanosponges for hydrogen storage. J. Mater. Chem. **22**(20), 10134–10143 (2012)
Serre, C., Bourrelly, S., Vimont, A., Ramsahye, N.A., Maurin, G., Llewellyn, P.L., Daturi, M., Filinchuk, Y., Leynaud, O., Barnes, P., Férey, G.: An explanation for the very large breathing effect of a metal–organic framework during CO_2 adsorption. Adv. Mater. **19**(17), 2246–2251 (2007)
Silvera, I.F.: The solid molecular hydrogens in the condensed phase: Fundamentals and static properties. Rev. Mod. Phys. **52**(2), 393–452 (1980)
Sips, R.: On the structure of a catalyst surface. II. J. Chem. Phys. **18**(8), 1024–1026 (1950)
Sips, R.: On the structure of a catalyst surface. J. Chem. Phys. **16**, 490–495 (1948)
Ströbel, R., Garche, J., Moseley, P.T., Jörissen, L., Wolf, G.: Hydrogen storage by carbon materials. J. Power Sources **159**(2), 781–801 (2006)
Tóth, J.: State equations of the solid-gas interface layers. Acta Chim. Hung. **69**, 311 (1971)
U.S. Department of Energy: In: Targets for Onboard Hydrogen Storage Systems for Light-Duty Vehicles, vol. 2012 (2009)
Wang, Q., Johnson, J.K.: Computer simulations of hydrogen adsorption on graphite nanofibers. J. Phys. Chem. B **103**(2), 277–281 (1998)
Wilson, M.C., Galwey, A.K.: Compensation effect in heterogeneous catalytic reactions including hydrocarbon formation on clays. Nature **243**(5407), 402–404 (1973)
Zhou, L., Yao, J., Wang, Y., Zhou, Y.: Estimation of pore size distribution by CO_2 adsorption and its application in physical activation of precursors. Chin. J. Chem. Eng. **8**(3), 279–282 (2000)
Zhou, W., Wu, H., Hartman, M.R., Yildirim, T.: Hydrogen and methane adsorption in metal–organic frameworks: a high-pressure volumetric study. J. Phys. Chem. C **111**(44), 16131–16137 (2007)